JCS ePress online publication date 8 September 2009

Axin2 controls bone remodeling through the β-catenin–BMP signaling pathway in adult mice

Ying Yan[1,*], Dezhi Tang[1,2,*], Mo Chen[1], Jian Huang[1], Rong Xie[1], Jennifer H. Jonason[1], Xiaohong Tan[1], Wei Hou[1,2], David Reynolds[1], Wei Hsu[3], Stephen E. Harris[4], J. Edward Puzas[1], Hani Awad[1,5], Regis J. O'Keefe[1], Brendan F. Boyce[6] and Di Chen[1,‡]

[1]Department of Orthopaedics, Center for Musculoskeletal Research, [3]Department of Biomedical Genetics, Center for Oral Biology, [5]Department of Biomedical Engineering and [6]Department of Pathology, University of Rochester School of Medicine, Rochester, NY 14642, USA
[2]Spine Research Institute, Shanghai University of Traditional Chinese Medicine, Shanghai 200032, China
[4]Department of Periodontics, University of Texas Health Science Center at San Antonio, San Antonio, TX 78229, USA
*These authors contributed equally to this work
‡Author for correspondence (di_chen@urmc.rochester.edu)

Accepted 26 July 2009
Journal of Cell Science 122, 3566-3578 Published by The Company of Biologists 2009
doi:10.1242/jcs.051904

Summary

To investigate the role of Wnt–β-catenin signaling in bone remodeling, we analyzed the bone phenotype of female *Axin2-lacZ* knockout (KO) mice. We found that trabecular bone mass was significantly increased in 6- and 12-month-old *Axin2* KO mice and that bone formation rates were also significantly increased in 6-month-old *Axin2* KO mice compared with wild-type (WT) littermates. In vitro studies were performed using bone marrow stromal (BMS) cells isolated from 6-month-old WT and *Axin2* KO mice. Osteoblast proliferation and differentiation were significantly increased and osteoclast formation was significantly reduced in *Axin2* KO mice. Nuclear β-catenin protein levels were significantly increased in BMS cells derived from *Axin2* KO mice. In vitro deletion of the *β-catenin* gene under *Axin2* KO background significantly reversed the increased alkaline phosphatase activity and the expression of osteoblast marker genes observed in *Axin2* KO BMS cells. We also found that mRNA expression of *Bmp2* and *Bmp4* and phosphorylated Smad1/5 protein levels were significantly increased in BMS cells derived from *Axin2* KO mice. The chemical compound BIO, an inhibitor of glycogen synthase kinase 3β, was utilized for in vitro signaling studies in which upregulated *Bmp2* and *Bmp4* expression was measured in primary calvarial osteoblasts. Primary calvarial osteoblasts were isolated from $Bmp2^{fx/fx};Bmp4^{fx/fx}$ mice and infected with adenovirus-expressing Cre recombinase. BIO induced *Osx*, *Col1*, *Alp* and *Oc* mRNA expression in WT cells and these effects were significantly inhibited in *Bmp2/4*-deleted osteoblasts, suggesting that BIO-induced *Osx* and marker gene expression were *Bmp2/4*-dependent. We further demonstrated that BIO-induced osteoblast marker gene expression was significantly inhibited by *Osx* siRNA. Taken together, our findings demonstrate that Axin2 is a key negative regulator in bone remodeling in adult mice and regulates osteoblast differentiation through the β-catenin–BMP2/4–*Osx* signaling pathway in osteoblasts.

Supplementary material available online at
http://jcs.biologists.org/cgi/content/full/122/19/3566/DC1

Key words: Axin2, β-catenin, BMP, Osteoblast, Bone remodeling

Introduction

The Wnt family consists of a number of small, cysteine-rich, secreted glycoproteins that are involved in the regulation of a variety of cellular activities that are crucial for development (Huelsken and Birchmeier, 2001; Moon et al., 2002; Westendorf et al., 2004). The canonical Wnt signaling pathway is mediated by a protein complex containing β-catenin, through regulation of β-catenin protein levels and its subcellular localization. In the absence of Wnts, β-catenin levels are kept in a steady state. Free β-catenin proteins are ubiquitylated and degraded by the 26S proteasome (Aberle et al., 1997). A multiprotein complex containing the kinases glycogen synthase kinase 3β (GSK-3β) and casein kinase 1 (CK1) along with scaffolding proteins Axis inhibition protein 1 (Axin1), Axin2, adenomatous polyposis coli (APC) and disheveled (Dsh) mediates the degradation of excess β-catenin. This complex phosphorylates specific amino acid residues on β-catenin, creating a docking site for the F-box protein/E3 ligase complex (Behrens et al., 1998; Jiang and Struhl, 1998). Therefore, inhibition of β-catenin phosphorylation prevents degradation of β-catenin, increases its cytoplasmic level, and facilitates its nuclear translocation. Signaling from Wnt proteins makes the complex release β-catenin, and allows it to move to the nucleus, where it interacts with TCF/LEF transcription factors to activate the expression of target genes (Staal and Clevers, 2000; Moon et al., 2002; Cliffe et al., 2003; Westendorf et al., 2004).

At the cell surface, Wnts interact with two classes of proteins: frizzled receptors and low-density-lipoprotein (LDL)-receptor-related protein 5 or 6 (LRP5/6). There are many genes encoding frizzled proteins, including ten in the human genome. Individual frizzled proteins probably have different affinities for various types of Wnt proteins. Wnt proteins can form a complex with both the cysteine-rich domain (CRD) of frizzled and with LRP5/6 simultaneously, leading to the formation of a dual-receptor complex (Bejsovec, 2000; Huelsken and Birchmeier, 2001). The intracellular portion of the receptors communicates this binding information and turns on the pathways that act on β-catenin inside the cell. Following Wnt binding, the intracellular tail of LRP5/6 binds Axin1 (or Axin2) and causes dissociation of β-catenin from its protein complex and activation of β-catenin signaling (Mao et al., 2001).

Axin1 and its homolog Axin2 are negative regulators of canonical Wnt signaling through promotion of β-catenin degradation (Behrens et al., 1998; Kikuchi, 1999; Peifer and Polakis, 2000). Axin1 has interaction sites for proteins involved in Wnt signal transduction, including β-catenin, GSK-3β, CK1, APC, Dsh and LRP5 (Luo and Lin, 2004). Significantly, Axin1 associates with β-catenin and protein kinases GSK-3β and CK1. In this complex, β-catenin is phosphorylated and degraded by the ubiquitin-proteasome pathway. Wnt binding recruits Axin1 to the receptor complex, where it binds the cytoplasmic domain of LRP5 (Cong et al., 2004; Hay et al., 2005; Mao et al., 2001). Axin1 is a central component of the canonical Wnt pathway and acts as a scaffold for the protein complex involved in β-catenin degradation.

Mouse *Axin2* cDNA encodes a protein of 840 amino acids (Axin2, also known as conductin). Several important binding domains in Axin2 have been mapped. Axin2 has a β-catenin-binding domain that is located in the central region of Axin2 protein (amino acids 396-465). Axin2 contains a N-terminal RGS (regulator of G protein signaling) domain (amino acids 78-200), a GSK-3β binding domain (amino acids 343-396) and a C-terminal sequence related to the protein Dsh (amino acids 783-833) (Behrens et al., 1998). Axin2 has been shown to mediate APC-induced β-catenin degradation. The Axin2 RGS domain binds the SAMP repeats of APC. A double mutant of β-catenin (W383A/R386A) does not bind APC but this mutant is still degraded by exogenous wild-type (WT) APC, indicating that APC does not need to bind directly to β-catenin to induce β-catenin degradation. A triple mutant β-catenin (W383A/R386A/H260A) does not bind APC or Axin2 and this mutant β-catenin is fully stable in the presence of exogenous WT APC (von Kries et al., 2000). These results demonstrate that Axin2 can link APC to β-catenin and mediate APC-induced β-catenin degradation.

Axin2 has 44% homology with Axin1 and its function is similar (Behrens et al., 1998; Chia and Costantini, 2005), but they have different expression patterns. Axin1 is widely expressed, whereas Axin2 is differentially expressed in various cells and tissues, and during different stages of maturation (Chia and Costantini, 2005; Yu et al., 2005). The deletion of the *Axin1* gene results in early embryonic mortality. Mice die at embryonic day 9.5 with forebrain truncation, neural tube defects and axis duplications (Zeng et al., 1997). Knock-in of the *Axin2* gene into the deleted *Axin1* gene rescues the phenotype of *Axin1*-deficient mice (Chia and Costantini, 2005). A *lacZ* knock-in allele that is a null allele of *Axin2* (*Axin2*$^{-/-}$) was generated by insertion of the *lacZ* cDNA into exon2 of the *Axin2* gene. The homozygous *Axin2* knockout (KO) mice are viable and fertile, but have craniofacial defects and premature closure of the cranial sutures due to increased β-catenin signaling (Yu et al., 2005). Nevertheless, despite some overlapping functions, Axin1 and Axin2 do not have redundant functions, which probably reflects their differential expression patterns.

Although canonical Wnt/β-catenin signaling plays a crucial role in controlling bone development, its role in bone remodeling remains poorly understood because either deletion of the β-catenin gene in a conventional method or tissue-specific manner often leads to embryonic lethality. Using the *Axin2* KO mice as a unique mouse model, we have investigated the role of the Axin2/β-catenin signaling pathway in bone remodeling. Our findings demonstrate that Axin2/β-catenin signaling targets *Bmp2/4*, regulates *Osx* expression and controls osteoblast differentiation in osteoblast progenitor or precursor cells.

Results

Age-related increase in bone mass in *Axin2* KO mice

To investigate changes in bone mass and bone microstructure, we analyzed the metaphyseal region of long bones (femora) of 2-, 6- and 12-month-old WT and *Axin2* KO mice using micro-CT imaging. No obvious changes in trabecular bone parameters were observed in long bones of 2-month-old *Axin2* KO mice compared with WT controls (data not shown). By contrast, a significant increase in bone volume (BV) and bone mineral density (BMD) was observed in 6- and 12-month-old *Axin2* KO mice (Fig. 1). No significant difference in bone parameters was observed between heterozygous *Axin2* KO mice and WT controls at these three time points (data not shown). These results suggest that Axin2 might play a dominant role in bone formation in older mice.

Trabecular bone structure was significantly denser and more robust in 6-month-old female *Axin2* KO mice. Specifically, the bone volume fraction (BVF; BV as a percentage of tissue volume, TV) was 61% higher (*Axin2* KO: 12.7±1.8% versus WT: 7.9±1.0%, $P<0.05$, $n=6$) (Fig. 1A,B) and bone mineral density (BMD = BMC/TV) was 31% higher (*Axin2* KO: 214±12 mg/cm^3 versus WT: 164±17 mg/cm^3, $P<0.05$, $n=6$) in the *Axin2* KO mice than WT controls (Fig. 1C). However, the structural model index (SMI) (a measure of the shape of trabeculae; 0 for plates and 3 for cylindrical rods) was significantly decreased in these mice versus WT controls (Fig. 1D), reflecting plate-like morphology of trabeculae in *Axin2* KO mice compared to the rod-like morphology in the WT mice. Trabecular number (Tb.N.) and trabecular thickness (Tb.Th) were significantly increased (by 16% and 15%, respectively) in the KO mice (Fig. 1E,F), reflecting increased trabecular volume of the *Axin2* KO phenotype. By contrast, trabecular separation (Tb.Sp.) was significantly decreased (17%) in *Axin2* KO mice (Fig. 1G) compared to WT controls. To determine the expression patterns of *Axin1* and *Axin2* in bone cells, we isolated bone marrow stromal (BMS) cells from 2- and 6-month-old wild-type (WT) C57BL/6J mice and examined age-related changes in *Axin1* and *Axin2* expression. We found that *Axin1* expression was reduced 47% and *Axin2* expression was increased ninefold in 6-month-old mice compared to that in 2-month-old mice (Fig. 1H,I).

The differences in BV and BMD were much more pronounced and significant by 12 months of age. The BVF was increased 250% (*Axin2* KO: 9.8±2.4% versus WT: 2.8±0.5%, $P<0.05$, $n=6$) (Fig. 1J,K) and BMD was increased 73% (*Axin2* KO: 171±26 mg/cm^3 versus WT: 99±8, $P<0.05$, $n=6$) in *Axin2* KO mice compared with WT controls (Fig. 1L). The SMI was decreased 42% in *Axin2* KO mice (Fig. 1M), again reflecting trabeculae that resembled plate-like morphology compared to the rod-like morphology of the WT trabeculae. The Tb.N. and the Tb.Th. were increased by 39 and 21%, respectively, and Tb.Sp. was decreased 24% in *Axin2* KO mice (Fig. 1N-P). Similar, but less marked changes were also found in 6- and 12-month-old male *Axin2* Ks mice (data not shown).

Increased bone mechanical strength in *Axin2* KO mice

Long-bone diaphyseal morphology was not found to be different between WT and *Axin2* KO femurs nor between tibia, using micro-CT cross-sectional imaging. Diaphyseal cross-sectional area, bending moments of inertia, outer diameter and BMD were not significantly different (Table 1), with the exception that *Axin2* KO femoral cortical thickness was 10% greater, whereas the outer medial-lateral diameter was 9% smaller ($P<0.05$). To determine the effect of Axin2 on bone mechanics, eight femurs from 12-month-

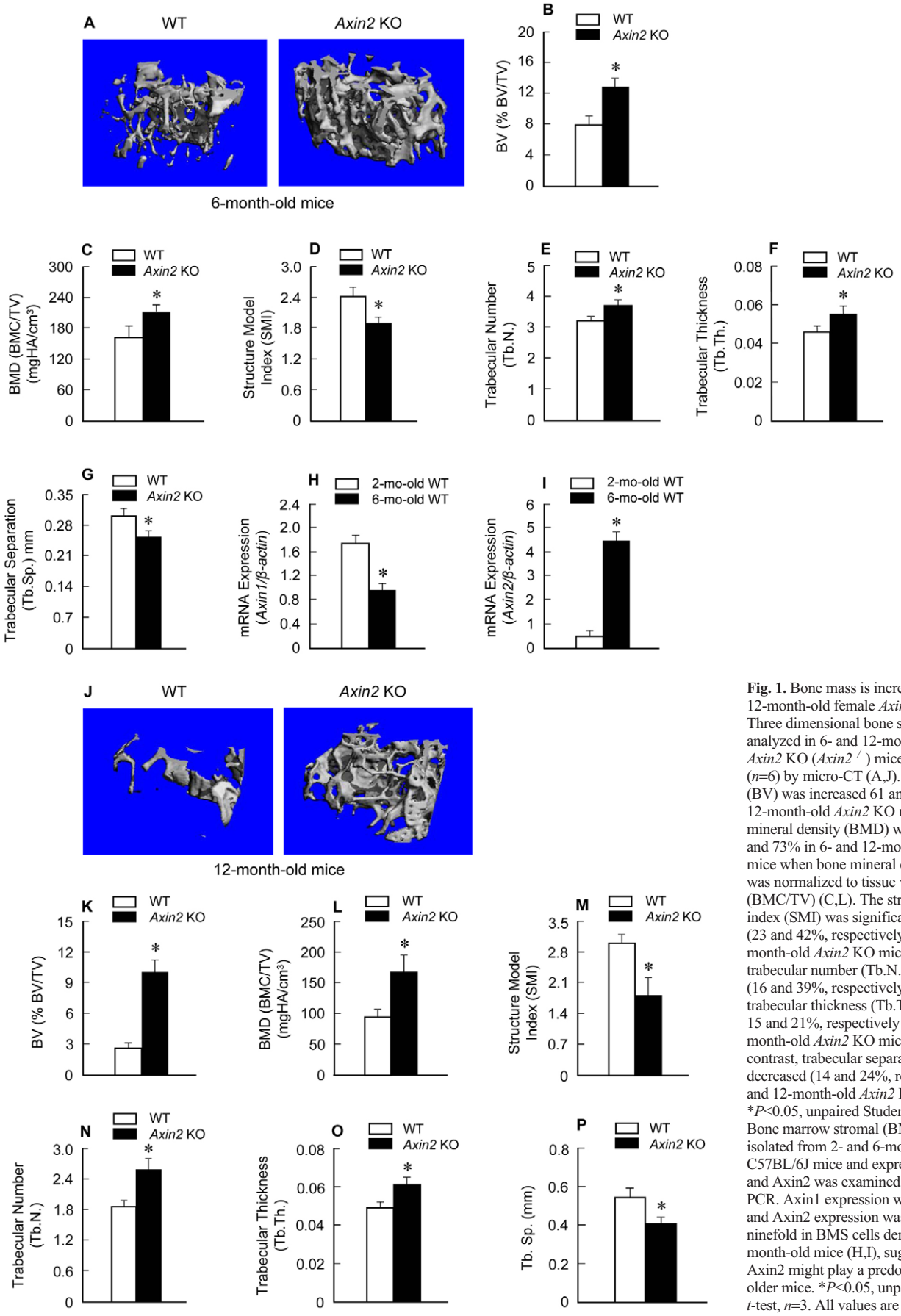

Fig. 1. Bone mass is increased in 6- and 12-month-old female *Axin2* KO mice. Three dimensional bone structure was analyzed in 6- and 12-month-old female *Axin2* KO (*Axin2*$^{-/-}$) mice and WT controls (n=6) by micro-CT (A,J). Bone volume (BV) was increased 61 and 255% in 6- and 12-month-old *Axin2* KO mice (B,K). Bone mineral density (BMD) was increased 30 and 73% in 6- and 12-month-old *Axin2* KO mice when bone mineral content (BMC) was normalized to tissue volume (BMC/TV) (C,L). The structural model index (SMI) was significantly decreased (23 and 42%, respectively) in 6- and 12-month-old *Axin2* KO mice (D,M). The trabecular number (Tb.N.) was increased (16 and 39%, respectively) (E,N) and trabecular thickness (Tb.Th.) was increased 15 and 21%, respectively in 6- and 12-month-old *Axin2* KO mice (F,O). By contrast, trabecular separation (Tb.Sp.) was decreased (14 and 24%, respectively) in 6- and 12-month-old *Axin2* KO mice (G,P). *P<0.05, unpaired Student's t-test, n=6. Bone marrow stromal (BMS) cells were isolated from 2- and 6-month-old WT C57BL/6J mice and expression of Axin1 and Axin2 was examined by real-time PCR. Axin1 expression was reduced 47% and Axin2 expression was increased ninefold in BMS cells derived from 6-month-old mice (H,I), suggesting that Axin2 might play a predominant role in older mice. *P<0.05, unpaired Student's t-test, n=3. All values are means ± s.e.

Table 1. Cross-sectional geometry of the mid femoral diaphysis from micro-CT imaging

Mouse type	Minimum bending moment of inertia (mm^4)	Maximum bending moment of inertia (mm^4)	Cross-sectional area (mm^2)	Cortical thickness (mm)	Maximum radius (mm)	Cortical BMD (mg HA/cm^3)
WT	0.169±0.004	0.282±0.022	0.928±0.021	0.211±0.012	0.94±0.05	1346±6
Axin2 KO	0.178±0.048	0.236±0.054	0.957±0.11	0.233±0.008*	0.86±0.05*	1368±23

Data presented as mean ± s.d. *P<0.05, unpaired Student's t-test. WT, wild-type littermates; KO knockout.

old WT and seven femurs from *Axin2* KO mice underwent three-point bending mechanical testing. Femurs from *Axin2* KO animals were significantly stiffer by 31%, with a maximum bending moment that was 20% greater (P<0.05, Table 2) than for WT controls.

Increased osteoblast function in *Axin2* KO mice

Consistent with the phenotypic changes measured by micro-CT, histological analysis also showed a significant increase in bone volume in 6- and 12-month-old female *Axin2* KO mice (Fig. 2A,B). The mineral appositional rates (MAR) and bone formation rates (BFR) were increased 64 and 86%, respectively, in 6-month-old female *Axin2* KO mice, as demonstrated by histomorphometric analysis (Fig. 2C,D). The micro-CT and histomorphometric results demonstrated a dramatic increase in bone mass in 6- and 12-month-old *Axin2* KO mice and suggest that Axin2 is a negative regulator in the maintenance of bone mass in adult mice. Because BFR is increased in *Axin2* KO mice, the data also suggest that osteoblast function is elevated in *Axin2* KO mice.

Reduced osteoclast formation in *Axin2* KO mice

To determine whether increased bone mass in *Axin2* KO mice is also due to a decrease in osteoclast formation, we also analyzed changes in osteoclast numbers. We found that osteoclast surfaces and osteoclast numbers were significantly reduced in 6-month-old *Axin2* KO mice (Fig. 2E,F). We also examined the ability of BMS cells to form osteoclasts in response to M-CSF (macrophage-colony stimulating factor) and RANKL (receptor activator for nuclear factor-kB ligand). The results showed that osteoclast formation was significantly reduced (n=4) in the cells derived from 6-month-old *Axin2* KO mice compared with formation in the cells obtained from WT controls under the same culture conditions (Fig. 2G,H). In addition, we also found that osteoclastic bone resorption was also significantly reduced in bone marrow cells derived from Axin2 KO mice (Fig. 2I). The mRNA expression of *osteoprotegerin* (*Opg*) in BMS cells was significantly increased in 6-month-old *Axin2* KO mice (Fig. 2J). By contrast, *Rankl* expression was slightly reduced in *Axin2* KO mice (Fig. 2K). In addition, the expression of *cathepsin K* was significantly reduced in *Axin2* KO mice (Fig. 2L). Consistent with the increased *Opg* mRNA expression, serum OPG protein levels were also significantly increased in *Axin2* KO mice (Fig. 2M). These results suggest that reduction in osteoclast formation and bone resorption might also contribute to the high-bone-mass phenotype observed in *Axin2* KO mice.

To determine the role of Axin2 in bone loss induced by estrogen deficiency, we performed an ovariectomy experiment in 6-month-old female *Axin2* KO mice and WT controls. The changes in bone volume were monitored by micro-CT analysis. There was 48% bone loss (BV/TV) in WT mice 4 weeks after ovariectomy compared with sham-operated mice (n=10). By contrast, only 36% bone loss was found in *Axin2* KO mice 4 weeks after ovariectomy (n=10) (supplementary material Fig. S1). These findings demonstrated that *Axin2* KO mice are partially resistant to overiectomy-induced bone loss and that this might be related to the increased *Opg* expression in *Axin2* KO mice.

Increases in osteoblast proliferation and differentiation in *Axin2* KO mice

To investigate changes in cellular function, we isolated BMS cells from 6-month-old *Axin2* KO mice and WT controls and cultured these cells for different periods of time. We first examined cell proliferation by immunostaining using an anti-Ki-67 antibody and found a significant increase in Ki-67-positive cells (5.7-fold increase) in BMS cells from *Axin2* KO mice (Fig. 3A) versus WT controls. It has been reported that β-catenin directly activates *cyclin D1* gene transcription in tumor cells (Tetsu and McCormick, 1999). We analyzed changes in *cyclin D1* expression and found that the expression of *cyclin D1* mRNA and protein was significantly increased in BMS cells derived from *Axin2* KO mice compared with that in WT BMS cells (Fig. 3B,C).

We determined changes in osteoblast differentiation by examining a panel of osteoblast maker genes expressed at various developmental stages using enzyme activity assay and real-time PCR assays. The alkaline phosphatase (ALP) activity (Fig. 3D,E) and the expression of osteoblast-specific transcription factors, *Runx2* and *osterix* (*Osx*), were significantly increased in BMS cells derived from 6-month-old *Axin2* KO mice (Fig. 3F,G). As a consequence, the expression of early osteoblast differentiation markers, *type I collagen* (*Col1*) and *osteopontin* (*Opn*) was also significantly increased in *Axin2* KO BMS cells (Fig. 3H,I). The expression levels of later-stage marker genes such as *bone sialoprotein* (*Bsp*) and *osteocalcin* (*Oc*) were also significantly increased in *Axin2* KO cells (Fig. 3J,K). These data suggest that osteoblast differentiation was largely advanced in the *Axin2* KO

Table 2. Biomechanical properties of mouse femurs from three-point bending

Mouse type	Stiffness (N/mm)	Yield bending moment (N mm)	Maximum bending moment (N mm)	Energy to max moment (N mm)
WT	119±8.3	50.4±8.82	68.5±14.4	3.46±0.77
Axin2 KO	156±16.0*	55.8±10.6*	82.5±8.76*	2.90±0.59

Data presented as mean ± s.d. *P<0.05, unpaired Student's t-test. WT, wild type littermates; KO knockout.

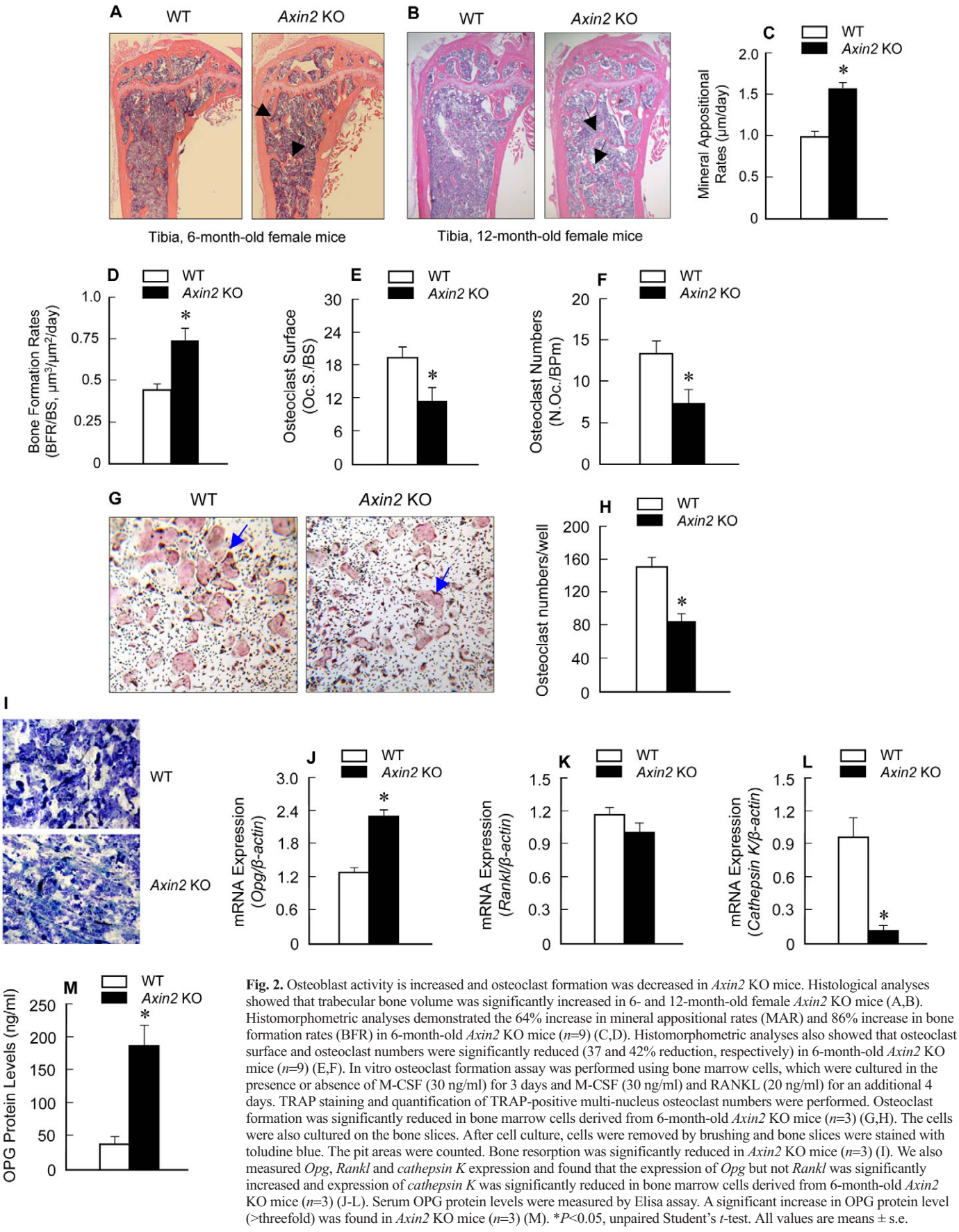

Fig. 2. Osteoblast activity is increased and osteoclast formation was decreased in *Axin2* KO mice. Histological analyses showed that trabecular bone volume was significantly increased in 6- and 12-month-old female *Axin2* KO mice (A,B). Histomorphometric analyses demonstrated the 64% increase in mineral appositional rates (MAR) and 86% increase in bone formation rates (BFR) in 6-month-old *Axin2* KO mice (n=9) (C,D). Histomorphometric analyses also showed that osteoclast surface and osteoclast numbers were significantly reduced (37 and 42% reduction, respectively) in 6-month-old *Axin2* KO mice (n=9) (E,F). In vitro osteoclast formation assay was performed using bone marrow cells, which were cultured in the presence or absence of M-CSF (30 ng/ml) for 3 days and M-CSF (30 ng/ml) and RANKL (20 ng/ml) for an additional 4 days. TRAP staining and quantification of TRAP-positive multi-nucleus osteoclast numbers were performed. Osteoclast formation was significantly reduced in bone marrow cells derived from 6-month-old *Axin2* KO mice (n=3) (G,H). The cells were also cultured on the bone slices. After cell culture, cells were removed by brushing and bone slices were stained with toludine blue. The pit areas were counted. Bone resorption was significantly reduced in *Axin2* KO mice (n=3) (I). We also measured *Opg*, *Rankl* and *cathepsin K* expression and found that the expression of *Opg* but not *Rankl* was significantly increased and expression of *cathepsin K* was significantly reduced in bone marrow cells derived from 6-month-old *Axin2* KO mice (n=3) (J-L). Serum OPG protein levels were measured by Elisa assay. A significant increase in OPG protein level (>threefold) was found in *Axin2* KO mice (n=3) (M). *P<0.05, unpaired Student's t-test. All values are means ± s.e.

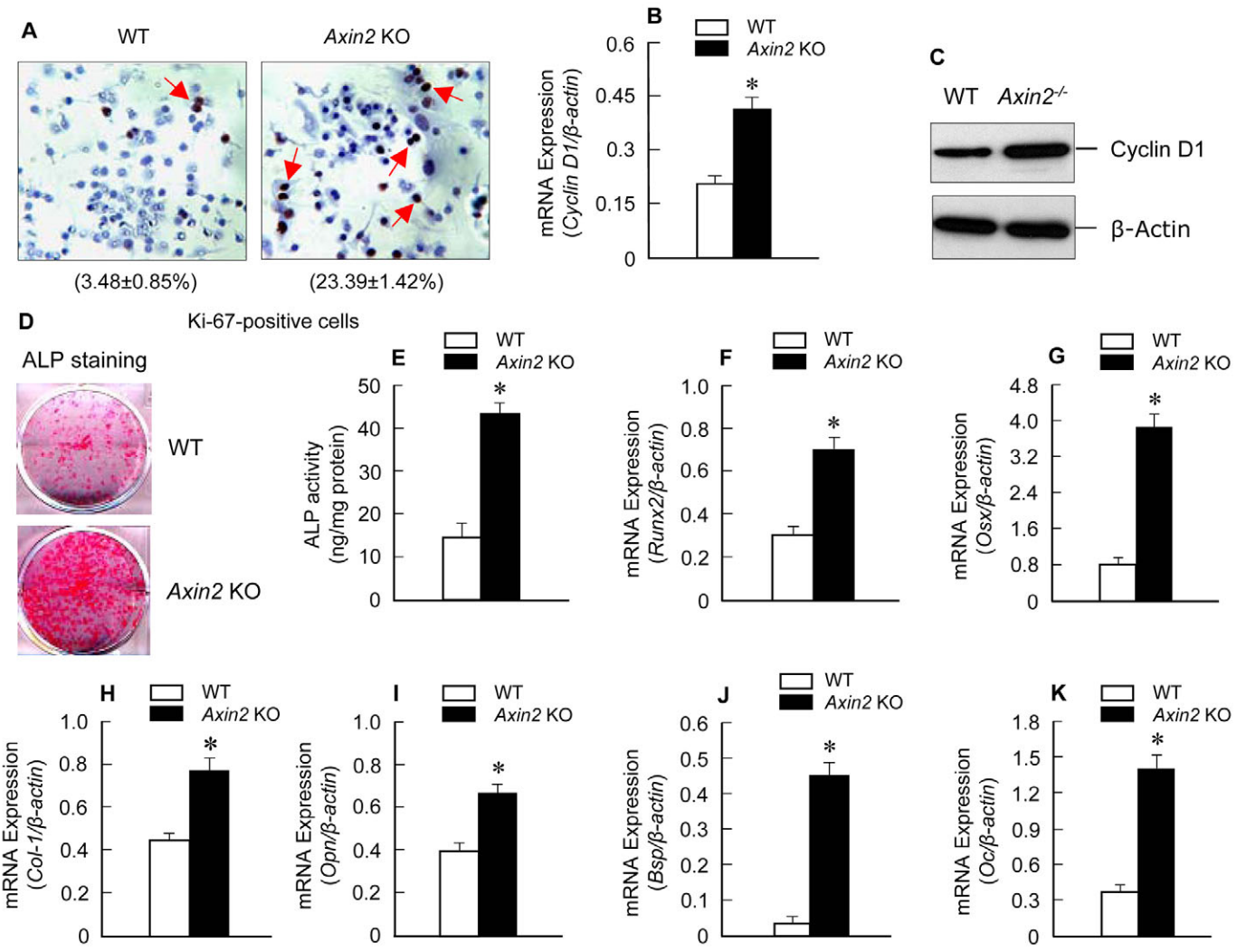

Fig. 3. Osteoblast proliferation and differentiation are increased in bone marrow stromal (BMS) cells of *Axin2* KO mice. BMS cells were isolated from 6-month-old WT and *Axin2* KO mice. Cells were cultured for 6 days and Ki-67 staining was performed. Ki-67-positive cells were increased 5.7-fold in BMS cells derived from *Axin2* KO mice (A). Consistent with this finding, cyclin D1 mRNA and protein expression were also increased in BMS cells derived from *Axin2* KO mice (B,C). **P*<0.05, unpaired Student's *t*-test, *n*=4. BMS cells were cultured for 10 days for ALP staining and activity assay. The intensity of ALP staining and ALP activity (1.8-fold increase) were significantly increased in BMS cells derived from 6-month-old *Axin2* KO mice (D,E). BMS cells were also cultured for 10 days and total RNA was extracted from the cells and expression of osteoblast marker genes was measured by real-time PCR assay. The expression of *Runx2*, *osterix* (*Osx*), *type I collagen* (*Col-1*), *osteopontin* (*Opn*), *bone sialoprotein* (*Bsp*) (G) and *osteocalcin* (*Oc*) (H) was significantly increased in BMS cells derived from *Axin2* KO mice (F-K). **P*<0.05, unpaired Student's *t*-test, *n*=3. All values are means ± s.e.

BMS cells. In contrast to the findings observed in BMS cells derived from 6-month-old *Axin2* KO mice, no significant changes in cell proliferation, ALP activity or the expression of osteoblast marker genes were found in BMS cells derived from 2-month-old *Axin2* KO mice (data not shown). Osteoblast apoptosis was examined by TUNEL staining and no changes in cell apoptosis were found between the *Axin2* KO and WT BMS cells from either 2- or 6-month-old mice (data not shown). These in vitro studies demonstrate that the process of osteoblast proliferation and differentiation is accelerated in the *Axin2* KO mice.

Activation of β-catenin signaling in *Axin2* KO mice

It has been reported that β-catenin promotes mesenchymal progenitor cells and osteoblast precursor cells to differentiate into osteoblasts (Hill et al., 2005; Day et al., 2005; Rodda and McMahon, 2006) and that it stimulates *Opg* expression in mature osteoblasts (Glass et al., 2005; Holmen et al., 2005). Because the phenotype found in *Axin2* KO mice is consistent with the phenotypes observed in mice with *β-catenin* gene deletions at the different stages of osteoblast lineages, we examined cytoplasmic and nuclear β-catenin protein levels to determine changes in β-catenin signaling in *Axin2* KO mice. Although the protein levels of β-catenin in cytoplasm were slightly increased, the protein levels of β-catenin (total and non-phosphorylated active form) in the nucleus were significantly increased in BMS cells derived from 6-month-old *Axin2* KO mice (Fig. 4A,B). These results suggest that the bone phenotype observed in *Axin2* KO mice could be due to the activation of β-catenin in osteoblasts.

To confirm the role of β-catenin activation in the bone phenotype of *Axin2* KO mice, we crossed *Axin2* KO mice with *β-catenin*$^{fx/fx}$ mice and generated *Axin2*$^{-/-}$;*β-catenin*$^{fx/fx}$ mice. BMS cells were then isolated from 6-month-old WT, *Axin2*$^{-/-}$, *β-*

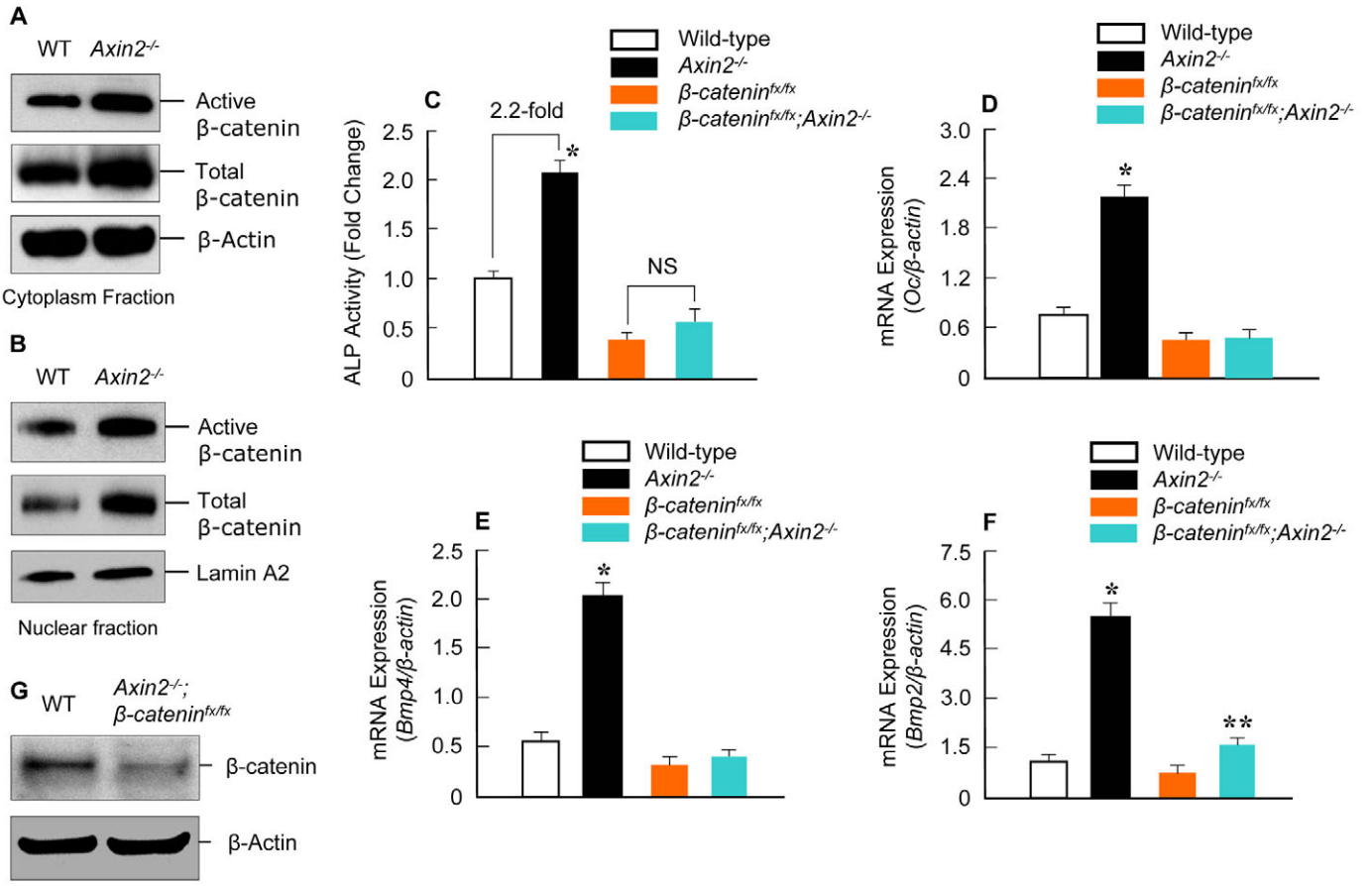

Fig. 4. Increased β-catenin levels are responsible for the bone phenotype observed in *Axin2* KO mice. Cell lysates (cytosolic and nuclear fractions) were collected from BMS cells isolated from 6-month-old WT and *Axin2* KO mice. Western blot assays were performed to examine changes in total and non-phosphorylated active form of β-catenin protein. Cytoplasm β-catenin levels (active and total) were slightly increased (A). By contrast, the nuclear β-catenin levels (active and total) were significantly increased in BMS cells derived from 6-month-old *Axin2* KO mice (B). *Axin2* KO mice were bred with *β-catenin*$^{fx/fx}$ mice to produce *Axin2*$^{-/-}$*;β-catenin*$^{fx/fx}$ mice. BMS cells were isolated from 6-month-old WT, *Axin2*$^{-/-}$, *β-catenin*$^{fx/fx}$ and *Axin2*$^{-/-}$*;β-catenin*$^{fx/fx}$ mice and were infected with lentivirus expressing Cre recombinase (Lenti-Cre). ALP activity and expression of *osteocalcin* (*Oc*) and *Bmp2* and *Bmp4* were examined. Deletion of the *β-catenin* gene by Lenti-Cre completely inhibited increased ALP activity (C) and *Oc* and *Bmp4* expression (D,E) and significantly inhibited *Bmp2* expression (F) observed in *Axin2* KO mice. Deletion of the *β-catenin* gene was determined by measuring levels of β-catenin protein using western blot analysis (G). **P*<0.05, unpaired Student's *t*-test, *n*=3. All values are means ± s.e.

catenin$^{fx/fx}$ and *Axin2*$^{-/-}$*;β-catenin*$^{fx/fx}$ mice and infected with lentivirus expressing Cre recombinase (Lenti-Cre). ALP activity and the expression of osteoblast marker genes were examined in these cells. The results showed that the increased ALP activity and increased *Bmp4* and *Oc* expression observed in *Axin2* KO mice were completely inhibited in *β-catenin*-deleted BMS cells under the *Axin2* KO background (Fig. 4C-E). In addition, the increased *Bmp2* expression found in *Axin2* KO mice was also significantly inhibited in β-catenin-deleted BMS cells (Fig. 4F). In vitro deletion of the *β-catenin* gene in BMS cells derived from 6-month-old *Axin2*$^{-/-}$*;β-catenin*$^{fx/fx}$ mice was confirmed by western blotting (Fig. 4G). These results strongly suggest that increased osteoblast function in *Axin2* KO mice is due to the activation of β-catenin in BMS cells.

Activation of BMP signaling in *Axin2* KO mice

The synergistic effect between β-catenin and bone morphogenetic protein (BMP) signaling in bone cells has been reported (Fischer et al., 2002; Mbalaviele et al., 2005; Nakashima et al., 2005; Chen et al., 2007). However, the mechanism remains unknown. To investigate the interaction between BMPs and Axin2 and/or β-catenin, we examined changes in expression levels of *Bmp*. We analyzed the mRNA levels of *Bmp* in BMS cells by real-time PCR. The results demonstrated that mRNA levels of *Bmp2 and Bmp4* were significantly increased in *Axin2* KO BMS cells (Fig. 5A,B). By contrast, the mRNA levels of *Bmp6* and *Bmp7* was not significantly changed in *Axin2* KO mice (data not shown). To determine whether signaling proteins downstream of BMP are activated in *Axin2* KO mice we measured changes in protein levels of phosphorylated Smad1/5, the key signaling molecules in BMP signaling. The basal levels of phosphorylated Smad1/5 (two BMP signaling Smads expressed in osteoblasts) were dramatically increased in the cells derived from 6-month-old *Axin2* KO mice. There was no change in the protein levels of total Smad1 (Fig. 5C), suggesting that the increased phosphorylated Smad1/5 level is not due to changes in protein degradation. In addition, BMP-2-induced formation of mineralized bone nodules was significantly enhanced in BMS cells derived from *Axin2* KO mice (13-fold increase for *Axin2* KO cells versus sixfold increase for WT cells) (Fig. 5D,E). Similar results were also obtained when BMS cells were incubated

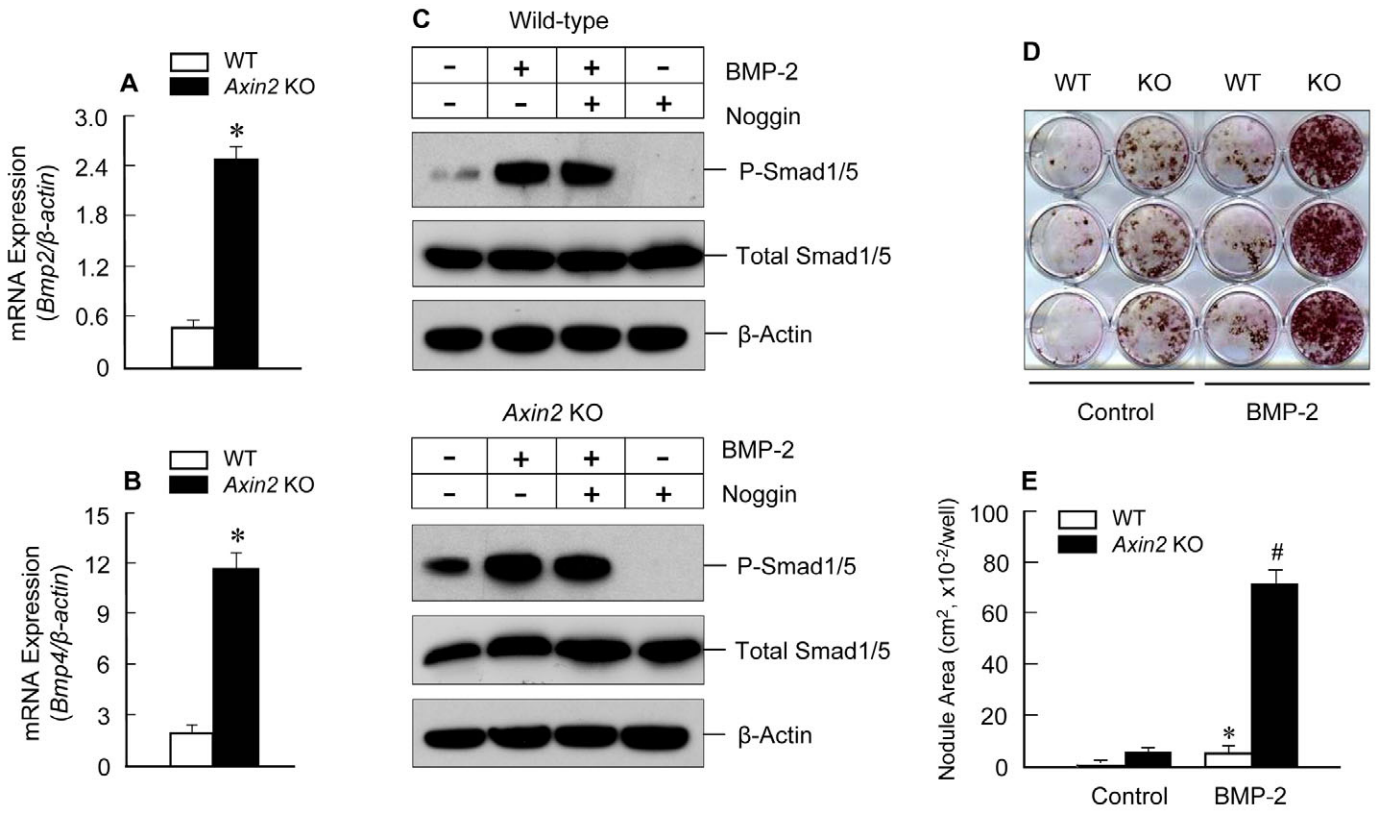

Fig. 5. BMP signaling is activated in *Axin2* KO mice. The mRNA expression of *Bmp2* and *Bmp4* was examined by real-time PCR using BMS cells derived from WT and *Axin2* KO mice. The expression of *Bmp2* and *Bmp4* was significantly increased in BMS cells derived from 6-month-old *Axin2* KO mice (A,B). Western blot assay was performed to analyze changes in phosphorylated Smad1/5 protein levels. The phosphorylated Smad1/5 was significantly increased in BMS cells derived from 6-month-old *Axin2* KO mice (C). In nodule formation assay, the responsiveness of the BMS cells to BMP-2 was higher in *Axin2* KO cells than WT cells (13-fold increase in *Axin2* KO cells versus sixfold increase in WT cells) (D,E). **P*<0.05, unpaired Student's *t*-test, *n*=3. All values are means ± s.e.

with BMP4 (data not shown). In contrast to the changes in BMP signaling, PTH-induced ALP activity was similar in the BMS cells from *Axin2* KO and WT mice (data not shown).

BIO-induced osteoblast differentiation is mediated by osterix

To further determine the regulatory mechanism of *Bmp* expression by Axin2 and β-catenin, we utilized the chemical compound BIO (6-bromoindirubin-3′-oxime), a GSK-3β inhibitor. BIO activated β-catenin signaling, stimulated ALP activity (Fig. 6A-D) and increased new bone formation in the periosteal bone formation assay in WT mice (Fig. 6E,F). BIO stimulated the expression of *Bmp2* and *Bmp4* genes over a 24-hour time period in primary osteoblasts (Fig. 7A,B). To determine whether BIO-induced osteoblast differentiation is dependent on *Bmp2/4*, primary calvarial osteoblasts were isolated from $Bmp2^{fx/fx};Bmp4^{fx/fx}$ mice and infected with adenovirus-expressing Cre recombinase (Ad-Cre). Infection of Ad-Cre in osteoblasts efficiently deleted *Bmp2* and *Bmp4* genes in these cells (Fig. 7C,D). BIO stimulated *Runx2* expression in both WT and *Bmp2/4*-deleted cells (Fig. 7E), suggesting that BIO-induced *Runx2* expression is *Bmp2/4*-independent. By contrast, BIO-induced *Osx* expression was significantly inhibited and BIO-induced *Col1*, *Alp* and *Oc* expression was completely abolished in *Bmp2/4*-deleted osteoblasts (Fig. 7F-I), suggesting that BIO-induced *Osx* and subsequent osteoblast marker gene expression are *Bmp2/4*-dependent.

To further determine the role of *Osx* in BIO-induced osteoblast differentiation, *Osx* RNAi was transfected into primary osteoblasts, which were subsequently treated with BIO. The results showed that BIO-induced expression of *Alp*, *Col1* and *Oc* was significantly or completely inhibited when *Osx* gene expression was knocked down by *Osx* siRNA (Fig. 7J-M). These results demonstrated that BIO (or activation of β-catenin signaling) activates *Osx* expression and subsequently regulates the expression of other osteoblast marker genes.

Discussion

Axin2 is a key regulator of bone remodeling

Osteoporosis is a major health threat for the elderly, particularly for postmenopausal women. It is characterized by low bone mass, induced by ineffective bone remodeling, which leads to an increased incidence of fractures and to higher morbidity and mortality in affected individuals. Bone remodeling, a dynamic process involving bone resorption followed by bone formation, takes place throughout life to maintain bone homeostasis. In osteoporotic patients, progressive bone loss with age could be due to increased bone resorption or inadequate bone formation, or to a combination of both. A better understanding of the mechanisms through which bone formation and resorption are controlled is therefore crucial in determining the pathogenesis of osteoporosis and identifying potential molecular targets for the development of new therapies for this debilitating disease.

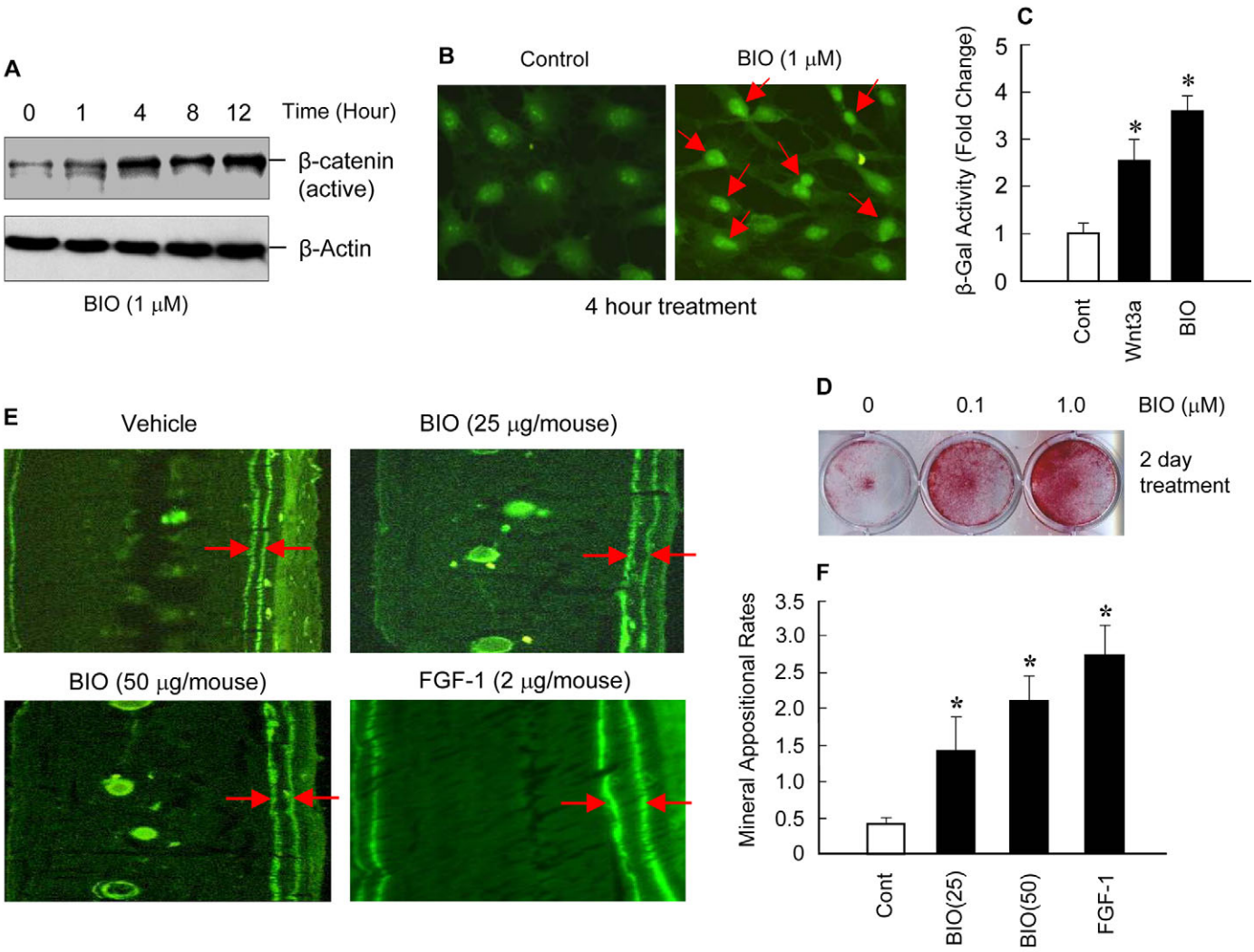

Fig. 6. BIO activates β-catenin signaling stimulates osteoblast differentiation and bone formation. Primary calvarial osteoblasts were isolated 3-day-old WT neonatal mice and cultured with or without BIO (1 μM) for different periods of time as indicated. The β-catenin protein levels and nuclear translocation were examined by western blot and immunostaining. BIO increased protein levels of active form of β-catenin and reached its maximal effect at 4 hours (A). BIO also induced β-catenin nuclear translocation (B). Primary calvarial osteoblasts, isolated from TOPGal transgenic mice, were treated with BIO (1 μM) for 24 hours and β-Gal activity was measured using cell lysates isolated from these cells. Wnt3a (100 ng/ml) was used as a positive control in this experiment. BIO significantly increased the β-Gal activity (C). *$P<0.05$, unpaired Student's *t*-test, $n=3$. Primary calvarial osteoblasts were cultured with 0.1 and 1 μM of BIO for 2 days and changes in ALP activity were examined by ALP staining. BIO (at both concentrations) significantly increased ALP activity in these cells (D). To further determine whether BIO induces new bone formation in vivo, 25 and 50 μg/mouse of BIO was injected into 1-month-old WT mice subcutaneously over the surface of calvariae for 5 days. Calcein labeling was performed at day 5 and 15. Mice were sacrificed 2 days after the second calcein labeling and periosteal new bone was evaluated and mineral appositional rates (MAR) were measured. FGF-1 (2 μg/mouse, 5 day injection) was used as a positive control. BIO significantly increased new bone formation and MAR in this assay (E,F). *$P<0.05$, one-way ANOVA followed by Dunnett's test (BIO versus control) and unpaired Student's *t*-test (FGF-1 versus control), $n=5$. All values are means ± s.e.

In the present studies, we discovered that bone mass is significantly increased in 6- and 12-month-old adult *Axin2* KO mice in which *lacZ* cDNA was inserted into exon2 of the *Axin2* gene and thereby effectively prevented *Axin2* expression in all cells of the mice (Yu et al., 2005). The present studies demonstrate for the first time that Axin2 plays a crucial role in the maintenance of bone mass in adult mice. Our in vivo results are complemented by cell-culture studies that show that osteoblast function is increased in vitro in cells from *Axin2* KO mice. We also found that mRNA expression of *Bmp2* and *Bmp4* and phosphorylated Smad1/5 protein levels are increased in *Axin2* KO BMS cells. These findings suggest an important cross-talk between the Axin2/β-catenin and BMP signaling pathways.

Axin2 inhibits osteoblast proliferation and differentiation

Axin2 is a scaffolding protein and a negative regulator of β-catenin function (Behrens et al., 1998). It has been reported that the N-terminal RGS domain of Axin2 binds to APC and mediates APC-induced β-catenin degradation (von Kries et al., 2000). In the present studies, we found that activation of β-catenin signaling is the major event in BMS cells of *Axin2* KO mice. β-catenin plays a crucial role in the commitment and differentiation of mesenchymal cells into the osteoblast lineage. Conditional deletion of the *β-catenin* gene in mesenchymal progenitor cells (targeted by *Prx1-Cre* or *Dermo1-Cre* mice) (Hill et al., 2005; Day et al., 2005) leads to the inhibition of osteoblast differentiation, suggesting that β-catenin promotes osteoblast differentiation in osteoblast progenitor cells.

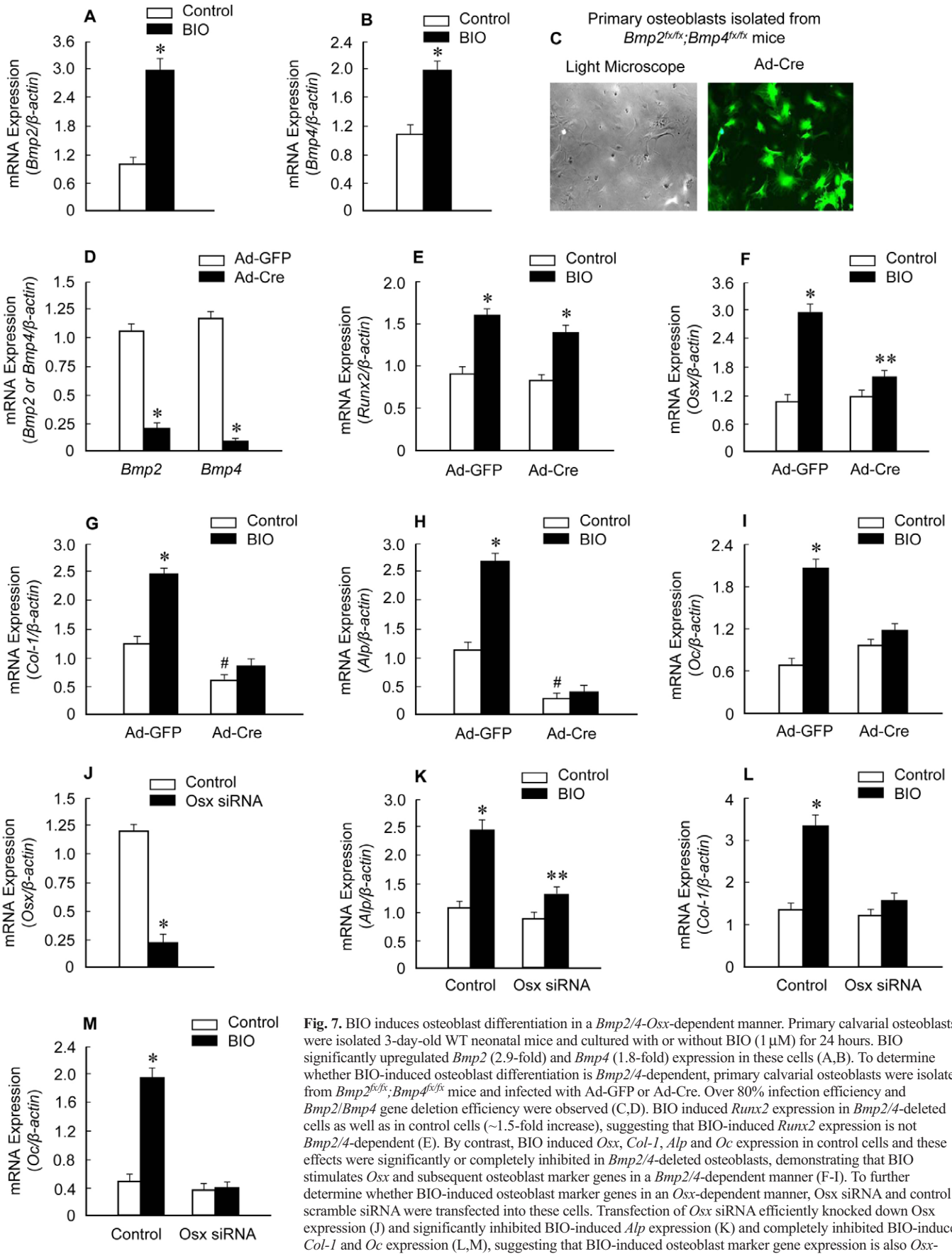

Fig. 7. BIO induces osteoblast differentiation in a *Bmp2/4-Osx*-dependent manner. Primary calvarial osteoblasts were isolated 3-day-old WT neonatal mice and cultured with or without BIO (1 μM) for 24 hours. BIO significantly upregulated *Bmp2* (2.9-fold) and *Bmp4* (1.8-fold) expression in these cells (A,B). To determine whether BIO-induced osteoblast differentiation is *Bmp2/4*-dependent, primary calvarial osteoblasts were isolated from $Bmp2^{fx/fx};Bmp4^{fx/fx}$ mice and infected with Ad-GFP or Ad-Cre. Over 80% infection efficiency and *Bmp2*/*Bmp4* gene deletion efficiency were observed (C,D). BIO induced *Runx2* expression in *Bmp2/4*-deleted cells as well as in control cells (~1.5-fold increase), suggesting that BIO-induced *Runx2* expression is not *Bmp2/4*-dependent (E). By contrast, BIO induced *Osx*, *Col-1*, *Alp* and *Oc* expression in control cells and these effects were significantly or completely inhibited in *Bmp2/4*-deleted osteoblasts, demonstrating that BIO stimulates *Osx* and subsequent osteoblast marker genes in a *Bmp2/4*-dependent manner (F-I). To further determine whether BIO-induced osteoblast marker genes in an *Osx*-dependent manner, Osx siRNA and control scramble siRNA were transfected into these cells. Transfection of *Osx* siRNA efficiently knocked down Osx expression (J) and significantly inhibited BIO-induced *Alp* expression (K) and completely inhibited BIO-induced *Col-1* and *Oc* expression (L,M), suggesting that BIO-induced osteoblast marker gene expression is also *Osx*-dependent. **P*<0.05, unpaired Student's *t*-test, *n*=3. All values are means ± s.e.

By contrast, continued activation of β-catenin signaling in *Osx1*$^{+}$ cells (targeted by *Osx1-Cre* mice) promotes cell differentiation in *Runx2*$^{+}$/*Osx1*$^{+}$ osteoblast precursor cells but arrests osteoblasts in a low *Oc* expressing stage (Rodda and McMahon, 2006). In the present studies, we found that nuclear β-catenin protein levels are increased and osteoblast proliferation and differentiation are accelerated in *Axin2* KO mice. The results from the rescue experiments further demonstrate that activation of β-catenin signaling is the primary cause for the bone phenotype of the *Axin2* KO mice. These results suggest that Axin2 regulates osteoblast function through β-catenin signaling in BMS cells, mainly through osteoblast precursor cells.

Axin2 promotes osteoclast formation

In the present studies, we found that *Opg* expression is increased in *Axin2* KO mice. By contrast, the expression of *Rankl* is not significantly altered. As a consequence, osteoclast formation is reduced in *Axin2* KO mice. Although it seems that changes in osteoblast function are more pronounced than those in osteoclast function, the decreased osteoclast formation might also contribute to the bone phenotype observed in *Axin2* KO mice. In mature osteoblasts, β-catenin specifically activates *Opg* expression and inhibits osteoclast formation (Holmen et al., 2005; Glass et al., 2005). In the present studies, we observed a significant increase in *Opg* expression and a decrease in osteoclast formation in BMS cells of *Axin2* KO mice. To further investigate whether Axin2 directly targets mature osteoblasts to regulate osteoclast formation and bone mass, we have recently generated *2.3Col1-Axin2* transgenic mice in which the expression of an *Axin2* transgene is driven by the 2.3 kb mouse type I collagen promoter. The bone phenotype of these mice (two independent lines) was analyzed by micro-CT and histological methods. We found that there were no significant changes in bone mass, bone microstructure and bone mechanical properties in 3-month-old *2.3Col1-Axin2* transgenic mice compared with the WT littermates (supplementary material Fig. S2). These results suggest that Axin2 might be mainly targeting osteoblast progenitor and precursor cells, instead of mature osteoblasts.

Axin2 inhibits *Bmp2* and *Bmp4* expression in osteoblasts

In these studies, we found that mRNA expression of *Bmp2* and *Bmp4* and levels of phosphorylated Smad1/5 proteins are significantly increased and addition of noggin, an antagonist of BMP-2 and BMP-4, completely blocks elevated phosphorylated Smad1/5 levels in *Axin2* KO BMS cells. Our in vitro studies further demonstrate that the GSK-3β inhibitor BIO induces osteoblast-specific transcription factor *Osx* and osteoblast marker genes in a *Bmp2/4*-dependent manner. These findings suggest that *Bmp2* and *Bmp4* are downstream mediators of Axin2/β-catenin signaling in osteoblast precursor cells and that the accelerated osteoblast differentiation observed in *Axin2* KO mice might be the result of the activation of BMP signaling in osteoblast precursor cells. Consistent with these findings, in a separate study, we found that Wnt3a induces the expression of hypertrophic marker gene *type X collagen* and this effect is completely blocked by addition of noggin to the cell cultures of primary chondrocytes (Chen et al., 2008), suggesting that the BMPs are downstream mediators of canonical Wnt signaling in chondrocytes. Previous studies have shown that *Axin2* KO mice have cranial bone defects, a phenotype resembling craniosynostosis in humans (Yu et al., 2005). Further, BMP signaling is activated in calvarial osteoblasts of *Axin2* KO mice (Liu et al., 2007). However, it remains to be determined whether osteoblast differentiation induced by *Axin2* deletion (or activation of β-catenin) is totally dependent on the activation of BMP signaling. Our evidence that deletion of the *Bmp2/4* genes abrogates the BIO-induced *Osx* and subsequent osteoblast marker gene expression suggests that *Axin2* deletion might trigger the β-catenin–Bmp2/4–osterix signaling pathway in osteoblast precursor cells.

It has been reported that β-catenin activates the bone-specific transcription factor Runx2 in osteoblasts and chondrocytes (Gaur et al., 2005; Dong et al., 2006). In the present studies, we found that both *Runx2* and *Osx* expression were increased in *Axin2* KO mice and that treatment with BIO in calvarial osteoblasts enhanced the expression of *Runx2*, *Osx* and other osteoblast marker genes. To determine whether BIO-induced osteoblast marker gene expression is *Bmp2/4*-dependent, primary calvarial osteoblasts were isolated from *Bmp2*$^{fx/fx}$;*Bmp4*$^{fx/fx}$ mice and infected with Ad-Cre and treated with BIO. We found that BIO-induced *Runx2* expression was not affected by deletion of the *Bmp2/4* genes. By contrast, deletion of the *Bmp2/4* genes significantly inhibited the BIO-induced *Osx* expression and completely abolished BIO-induced expression of other osteoblast marker genes. We further demonstrated that Osx siRNA also inhibited BIO-induced osteoblast marker gene expression. These observations suggest that BIO (or activation of β-catenin signaling) might stimulate osteoblast differentiation through a *Bmp2/4-Osx* pathway.

Axin2 inhibits Smad1/5 phosphorylation in osteoblasts

In the present studies, we found a significant increase in the levels of phosphorylated Smad1/5 in BMS cells derived from *Axin2* KO mice. A possible mechanism for this could be increased Smad1/5 phosphorylation or decreased Smad1/5 dephosphorylation. Three different types of phosphatases have recently been identified to specifically induce Smad1/5 dephosphorylation. These are pyruvate dehydrogenase phosphatase 1 and 2 (PDP1 and PDP2), small C-terminal domain phosphatase (SCP) and magnesium-dependent protein phosphatase 1α (PPM1α) (Chen et al., 2006; Knockaert et al., 2006; Duan et al., 2006). We have obtained expression plasmids of these phosphatases from different collaborators and tested the effects of Axin2 on Smad1/5 dephosphorylation induced by these phosphatases. We found that PPM1A is the most potent phosphatase for inducing Smad1/5 dephosphorylation in BMS cells. However, Axin2 (or Axin1) could not prevent or delay Smad1/5 dephosphorylation in BMS cells (supplementary material Fig. S3). It has been recently reported that GSK-3β can phosphorylate the linker domain of Smad1, leading to Smad1 polyubiquitylation (Fuentealba et al., 2007). We have looked at whether Axin2 regulates Smad1 levels through affecting the phosphorylation of the linker domain of Smad1 and found that Axin2 has no effect on Smad1 linker domain phosphorylation in 2T3 cells (supplementary material Fig. S4). In addition, the total Smad1 protein levels were not changed in *Axin2* KO BMS cells. These results demonstrate that the increase in Smad1 phosphorylation level is due to increased *Bmp* expression but not to a decrease in Smad1 dephosphorylation or linker domain phosphorylation of Smad1.

Conclusions

In summary, our findings demonstrate for the first time that Axin2 is a crucial negative regulator of bone remodeling in adult mice. Deletion of the *Axin2* gene causes an age-dependent high-bone-mass phenotype. In *Axin2* KO mice, β-catenin signaling is activated; osteoblast proliferation and differentiation are accelerated; and *Opg* expression is increased and leads to decreased osteoclast formation.

We also discovered that BMPs are downstream mediators of Axin2/β-catenin signaling in osteoblast precursor cells, suggesting an important cross-talk between β-catenin and BMP signaling in the regulation of osteoblast differentiation. Our findings suggest that Axin2 might be an important therapeutic target for modulation of bone homeostasis.

Materials and Methods

Mouse strains and genotyping

The *Axin2*$^{-/-}$ mice and genotyping method were reported previously (Yu et al., 2005). A pair of upper (5′-AGTCCATCTTCATTCCGCCTAGC-3′) and lower (5′-TGGTAATGCTGCAGTGGCTTG-3′) primers were used to detect WT *Axin2* and another pair of upper (5′-AGTCCATCTTCATTCCGCCTAGC-3′) and lower (5′-AAGCTGCGTCGGATACTTGCGA-3′) primers were used to detect the *Axin2*$^{-/-}$ allele. The Catnb^{tm2Kem}/J strain (Brault et al., 2001) carrying a floxed allele of *β-catenin* was obtained from Jackson Laboratory.

Micro-CT analysis

Quantitative analysis was performed in bone samples of femora from WT and *Axin2* KO mice (6- and 12-month-old) at 10-μM resolution on a micro-CT Scanner (VivaCT 40; Scanco Medical AG, Bassersdorf, Switzerland) (Hildebrand et al., 1999). Briefly, scanning in the femora began approximately at the lower growth plate and extended proximally for 350 slices (each 10-μm thick). Morphometric analysis was performed on 150 slices extending proximally, beginning with the first slice in which the femoral condyles have fully merged. The trabecular bone is segmented from the cortical shell manually on key slices using a contouring tool, and the contours are morphed automatically to segment the trabecular bone on all slices. The three-dimensional structure and morphometry was constructed and analyzed. These parameters include BV/TV (%), BMD (mg HA/mm^3), Tb.N. (mm^{-1}), Tb.Th. (mm) and Tb.Sp. (mm) and SMI. Tb.Th., Tb.N. and Tb.Sp., are computed using algorithms that do not rely on assumptions about the underlying trabecular structure. Micro CT imaging was also performed in the mid diaphysis of the femur. Midshaft evaluation of 100 slices (1.0 mm) was performed to quantify the cross-sectional area, maximum and minimum bending moments of inertia, cortical thickness and maximum and minimum external radii, and cortical bone mineral density.

Mechanical testing

Changes in mechanical properties of the femoral shaft were determined using three-point bending mechanical testing. Testing was performed using an Instron Dynamite 8841 servo-hydraulic materials testing device equipped with a 1 kN load cell, with control and data collection using Bluehill software version 1.8 (Instron, Norwood, MA). Prior to testing, each femur was harvested and cleaned of soft-tissue and soaked in PBS for 3 hours to ensure hydration (Broz et al., 1993). The anterior surface of each femur was placed on the two support beams, which were separated by an 8-mm span. The femora were bent about the medial-lateral axis at a rate of 5 mm/minute (Jamsa et al., 1998). Force versus deformation data were collected and analyzed to calculate the bending stiffness (N/mm), yield bending moment (N mm), maximum bending moment (N mm) and toughness to maximum bending moment (N mm).

Histological and histomorphometric analysis

Detail methods for histological and histomorphometric analyses have been described previously (Zhao et al., 2002; Zhao et al., 2004). Histomorphometric analyses were performed on proximal tibial metaphyses in 6-month-old mice. The trabecular bone volume was quantified in the entire area of the bone marrow cavity 0.4–1.4 mm underneath the growth plates and expressed as a percentage of tissue volume. Histomorphometric analysis was performed using the OsteoMeasure system (OsteoMetrics, Atlanta, GA).

In vitro osteoclast formation assay

Bone marrow cells were isolated from femur and tibia of 6-month-old *Axin2*$^{-/-}$ mice and WT littermates and cultured with minimum essential medium (α-MEM) supplemented with 10% fetal bovine serum (FBS) in six-well culture plates and treated with M-CSF (30 ng/ml) (R&D) for 3 days and then cultured in 96-well culture plates at the density of 3×10^5/ml (200 μl per well). Cells were then treated with M-CSF (30 ng/ml) and RANKL (30 ng/ml) (R&D) for additional 4 days. Tartrate-resistant acid phosphatase (TRAP) staining was performed and the numbers of TRAP-positive multi-nuclear (≥3 nucleus) osteoclasts were counted.

Ki-67 staining

BMS cells isolated from 6-month-old WT and *Axin2*$^{-/-}$ mice were plated in a four-well chamber slide at a density of 1×10^6 cells per well and cultured with α-MEM supplemented with 10% FBS at 37°C for 6 days. The cells were fixed with cold methanol for 5 minutes, endogenous peroxidase quenched with 3% hydrogen peroxide for 20 minutes to block the non-specific binding site and then blocked with 1:20 normal goat serum for 20 minutes. The slides were incubated with 1:20 dilution of rabbit anti-Ki-67 antibody (Lab Vision Corp.) overnight at 4°C and then with 1:200 goat anti-rabbit IgG (Cell Signaling) for 30 minutes, and with 1:250 horseradish peroxidase streptavidin for 30 minutes. The slides were treated with deionized water mixed with 1 drop of Tween 20, and the color reaction with Romulin AEC Chromagen detected for 3-5 minutes. The hematoxylin counterstain was then performed. The nuclei of Ki-67-positive cells showed a dark brown color.

ALP activity and nodule formation

BMS cells or primary calvarial osteoblasts were fixed in 10% formalin. ALP staining was performed by 0.1% fast red salt (Sigma-Aldrich) (buffered with 0.05% Napthol AS-MX phosphate disodium salt, 2.8% *N*,*N*-dimethyl formamide, 0.1 M Tris maleate buffer, pH 8.4) at 37°C for 30 minutes. The assays for ALP activity and nodule formation were described in previous studies (Zhao et al., 2002; Zhao et al., 2004).

Real-time PCR

Details of the method for real-time PCR assay were previously described (Chen et al., 2008; Zhu et al., 2008; Zhang et al., 2009). β-actin was amplified as an internal control. Relative amounts of mRNA were normalized to β-actin and calculated using the software program Microsoft Excel. The primers were: Runx2 (5′-TCCTG-TAGATCCGAGCACCA-3′ and 5′-CTGCTGCTGTTGTTGCTGTT-3′), osteopontin (OPN) (5′-CATTGCCTCCTCCCTCCCGGTG-3′ and 5′-GTCATCACCTCGGC-CGTTGGGG-3′), type I Collagen (Col-1) (5′-CCTGGTAAAGATGGGCC-3′ and 5′-CACCAGGTTCACCTTTCGCACC-3′), ALP (5′-TGACCTTCTCTCCTC-CATCC-3′ and 5′-CTTCCTGGGAGTCTCATCCT-3′), osteocalcin (Oc) (5′-CTTGAAGACCGCCTACAAAC-3′ and 5′-GCTGCTGTGACATCCATAC-3′), bone sialoprotein (BSP) (5′-GAGCCAGGACTGCCGAAAGGAA-3′ and 5′-CCGTTGTCTCCTCCGCTGCTGC-3′), Bmp2 (5′-ACTTTTCTCGTTTGTGGAGC-3′ and 5′-GAACCCAGGTGTCTCCAAGA-3′), Bmp4 (5′-TGAGCCTTTCCAG-CAAGTTT-3′ and 5′-CTTCCCGGTCTCAGGTATCA-3′) and β-actin (5′-TGTT-ACCAACTGGGACGACGACA-3′ and 5′-CTGGGTCATCTTTTCACGGT-3′).

Western blot analysis

Details of the method for western blotting were described in previous studies (Shen et al., 2006a; Shen et al., 2006b; Zhang et al., 2009). Cyclin D1 mouse monoclonal antibodies (1:1000) (Cell Signaling), anti-β-catenin mouse monoclonal antibody (clone E-5) (1:1000) (Santa Cruz Biotechnology, Santa Cruz, CA), anti-active-β-catenin (anti-ABC) mouse monoclonal antibody (clone 8E7) (1:500) (Upstate Cell Signaling Solutions, Lake Placid, NY), anti-p-Smad1(Ser463/465)/Smad5 (Ser463/465)/Smad8 (Ser426/428) monoclonal antibody (1:1000) (Cells Signaling), anti-lamin-B1 mouse monoclonal antibody (1:400) (Santa Cruz Biotechnology) and anti-β-actin mouse monoclonal antibody (1:3000) (Sigma-Aldrich) were used as primary antibodies.

Lenti-Cre infection and Zeocin selection

HFPW-Cre and lentivirus packaging vectors were kindly provided by Eric Brown (University of Pennsylvania, Philadelphia, PA). Lenti-Cre virus was produced in the HEK 293FT cell line with the Virapower Trex Lenti-viral Expression System (Invitrogen) according to the manufacturer's protocol. Lenti-Cre condition media were kept at –80°C until used. BMS cells were infected with Lenti-Cre condition media for 7 days and then cultured with α-MEM containing Zeocin (Invitrogen, 20 μg/ml). At the end of the cell culture, mRNA was extracted and expression of osteoblast marker genes was examined by real-time PCR.

In vivo periosteal bone formation assay

BIO and fibroblast growth factor (FGF-1) were obtained from Calbiochem. FGF-1 was dissolved in PBS containing 0.1% BSA and was used as a positive control. BIO was dissolved in Corn Oil (Sigma) at 1 mg/ml. BIO was injected subcutaneously over the parietal bone of the calvariae of one-month-old C57BL/6J WT mice. Mice received either vehicle (corn oil alone) or BIO (25 and 50 μg/mouse) and FGF-1 (2 μg/mouse) daily for 5 days. Calcein (20 mg/kg i.p.) labeling was performed at days 7 and 14 and mice were sacrificed 2 days after the second label. At the end of the experiments, calvarial bones were removed, fixed in 75% ethanol, and embedded in plastic. Transverse sections were cut at 3-μm thickness and unstained sections were viewed under fluorescent microscope. Mineral appositional rates (MAR) were measured using the OsteoMeasure system (OsteoMetrics, Atlanta, GA).

Statistical analysis

For comparisons between two data groups the unpaired Student's *t*-test was used. For multiple comparisons between more than two groups, data was analyzed by one-way analysis of variance (ANOVA), followed by Dunnett's test. Differences were considered significant when a P value was less than 0.05.

This publication was made possible by Grant Numbers R01 AR051189, K02 AR052411, R01 AR054465 and R01 AR055915 from National Institute of Health (to D.C.) and Grant Number N08G-070 from New York State Department of Health and the Empire State Stem Cell Board (to D.C.). J.H.J. was sponsored by NIAMS T32-AR053459 training grant. We would like to thank Xinhua Feng (Baylor College of Medicine, Houston, TX) for providing the PPM1A expression

plasmid and Edward De Robertis (University of California, Los Angeles, CA) for providing us the anti-pSmad1^{GSK} antibody. Authors have no conflict of interest. Deposited in PMC for release after 12 months.

References

Aberle, H., Bauer, A., Stappert, J., Kispert, A. and Kemler, R. (1997). Beta-catenin is a target for the ubiquitin-proteasome pathway. *EMBO J.* **16**, 3797-3804.

Behrens, J., Jerchow, B. A., Wurtele, M., Grimm, J., Asbrand, C., Wirtz, R., Kuhl, M., Wedlich, D. and Birchmeier, W. (1998). Functional interaction of an axin homolog, conductin, with beta-catenin, APC, and GSK3beta. *Science* **280**, 596-599.

Bejsovec, A. (2000). Wnt signaling: an embarrassment of receptors. *Curr. Biol.* **10**, R919-R922.

Brault, V., Moore, R., Kutsch, S., Ishibashi, M., Rowitch, D. H., McMahon, A. P., Sommer, L., Boussadia, O. and Kemler, R. (2001). Inactivation of the beta-catenin gene by Wnt1-Cre-mediated deletion results in dramatic brain malformation and failure of craniofacial development. *Development* **128**, 1253-1264.

Broz, J. J., Simske, S. J., Greenberg, A. R. and Luttges, M. W. (1993). Effects of rehydration state on the flexural properties of whole mouse long bones. *J. Biomech. Eng.* **115**, 447-449.

Chen, H. B., Shen, J., Ip, Y. T. and Xu, L. (2006). Identification of phosphatases for Smad in the BMP/DPP pathway. *Genes Dev.* **20**, 648-653.

Chen, M., Zhu, M., Awad, H., Sheu, T., Boyce, B. F., Chen, D. and O'Keefe, R. J. (2008). Inhibition of β-catenin signaling causes defects in postnatal cartilage development. *J. Cell Sci.* **121**, 1455-1465.

Chen, Y., Whetstone, H. C., Youn, A., Nadesan, P., Chow, E. C., Lin, A. C. and Alman, B. A. (2007). Beta-catenin signaling pathway is crucial for bone morphogenetic protein 2 to induce new bone formation. *J. Biol. Chem.* **282**, 526-533.

Chia, I. V. and Costantini, F. (2005). Mouse axin and axin2/conductin proteins are functionally equivalent in vivo. *Mol. Cell. Biol.* **25**, 4371-4376.

Cliffe, A., Hamada, F. and Bienz, M. (2003). A role of Dishevelled in relocating Axin to the plasma membrane during wingless signaling. *Curr. Biol.* **13**, 960-966.

Cong, F., Schweizer, L. and Varmus, H. (2004). Wnt signals across the plasma membrane to activate the beta-catenin pathway by forming oligomers containing its receptors, Frizzled and LRP. *Development* **131**, 5103-5115.

Day, T. F., Guo, X., Garrett-Beal, L. and Yang, Y. (2005). Wnt/beta-catenin signaling in mesenchymal progenitors controls osteoblast and chondrocyte differentiation during vertebrate skeletogenesis. *Dev. Cell* **8**, 739-750.

Dong, Y. F., Soung, Do. Y., Schwarz, E. M., O'Keefe, R. J. and Drissi, H. (2006). Wnt induction of chondrocyte hypertrophy through the Runx2 transcription factor. *J. Cell Physiol.* **208**, 77-86.

Duan, X., Liang, Y. Y., Feng, X. H. and Lin, X. (2006). Protein serine/threonine phosphatase PPM1A dephosphorylates Smad1 in the bone morphogenetic protein signaling pathway. *J. Biol. Chem.* **281**, 36526-36532.

Fischer, L., Boland, G. and Tuan, R. S. (2002). Wnt-3A enhances bone morphogenetic protein-2-mediated chondrogenesis of murine C3H10T1/2 mesenchymal cells. *J. Biol. Chem.* **277**, 30870-30878.

Fuentealba, L. C., Eivers, E., Ikeda, A., Hurtado, C., Kuroda, H., Pera, E. M. and De Robertis, E. M. (2007). Integrating patterning signals: Wnt/GSK3 regulates the duration of the BMP/Smad1 signal. *Cell* **131**, 980-993.

Gaur, T., Lengner, C. J., Hovhannisyan, H., Bhat, R. A., Bodine, P. V., Komm, B. S., Javed, A., van Wijnen, A. J., Stein, J. L., Stein, G. S. et al. (2005). Canonical WNT signaling promotes osteogenesis by directly stimulating Runx2 gene expression. *J. Biol. Chem.* **280**, 33132-33140.

Glass, D. A., 2nd., Bialek, P., Ahn, J. D., Starbuck, M., Patel, M. S., Clevers, H., Taketo, M. M., Long, F., McMahon, A. P., Lang, R. A. et al. (2005). Canonical Wnt signaling in differentiated osteoblasts controls osteoclast differentiation. *Dev. Cell* **8**, 751-764.

Hay, E., Faucheu, C., Suc-Royer, I., Touitou, R., Stiot, V., Vayssiere, B., Baron, R., Roman-Roman, S. and Rawadi, G. (2005). Interaction between LRP5 and Frat1 mediates the activation of the Wnt canonical pathway. *J. Biol. Chem.* **280**, 13616-13623.

Hildebrand, T., Laib, A., Muller, R., Dequeker, J. and Ruegsegger, P. (1999). Direct three-dimensional morphometric analysis of human cancellous bone: microstructural data from spine, femur, iliac crest, and calcaneus. *J. Bone Miner. Res.* **14**, 1167-1174.

Hill, T. P., Später, D., Taketo, M. M., Birchmeier, W. and Hartmann, C. (2005). Canonical Wnt/beta-catenin signaling prevents osteoblasts from differentiating into chondrocytes. *Dev. Cell* **8**, 727-738.

Holmen, S. L., Zylstra, C. R., Mukherjee, A., Sigler, R. E., Faugere, M. C., Bouxsein, M. L., Deng, L., Clemens, T. L. and Williams, B. O. (2005). Essential role of beta-catenin in postnatal bone acquisition. *J. Biol. Chem.* **280**, 21162-21168.

Huelsken, J. and Birchmeier, W. (2001). New aspects of Wnt signaling pathways in higher vertebrates. *Curr. Opin. Genet. Dev.* **11**, 547-553.

Jamsa, T., Jalovaara, P., Peng, Z., Vaananen, H. K. and Tuukkanen, J. (1998). Comparison of three-point bending test and peripheral quantitative computed tomography analysis in the evaluation of the strength of mouse femur and tibia. *Bone* **23**, 155-161.

Jiang, J. and Struhl, G. (1998). Regulation of the Hedgehog and Wingless signalling pathways by the F-box/WD40-repeat protein Slimb. *Nature* **391**, 493-496.

Kikuchi, A. (1999). Modulation of Wnt signaling by Axin and Axil. *Cytokine Growth Factor Rev.* **10**, 255-265.

Knockaert, M., Sapkota, G., Alarcon, C., Massague, J. and Brivanlou, A. H. (2006). Unique players in the BMP pathway: small C-terminal domain phosphatases dephosphorylate Smad1 to attenuate BMP signaling. *Proc. Natl. Acad. Sci. USA* **103**, 11940-11945.

Liu, B., Yu, H. M. and Hsu, W. (2007). Craniosynostosis caused by Axin2 deficiency is mediated through distinct functions of beta-catenin in proliferation and differentiation. *Dev. Biol.* **301**, 298-308.

Luo, W. and Lin, S. C. (2004). Axin: a master scaffold for multiple signaling pathways. *Neurosignals* **13**, 99-113.

Mao, J., Wang, J., Liu, B., Pan, W., Farr, G. H., 3rd., Flynn, C., Yuan, H., Takada, S., Kimelman, D., Li, L. et al. (2001). Low-density lipoprotein receptor-related protein-5 binds to Axin and regulates the canonical Wnt signaling pathway. *Mol. Cell* **7**, 801-809.

Mbalaviele, G., Sheikh, S., Stains, J. P., Salazar, V. S., Cheng, S. L., Chen, D. and Civitelli, R. (2005). Beta-catenin and BMP-2 synergize to promote osteoblast differentiation and new bone formation. *J. Cell. Biochem.* **94**, 403-418.

Moon, R. T., Bowerman, B., Boutros, M. and Perrimon, N. (2002). The promise and perils of Wnt signaling through beta-catenin. *Science* **296**, 1644-1646.

Nakashima, A., Katagiri, T. and Tamura, M. (2005). Cross-talk between Wnt and bone morphogenetic protein 2 (BMP-2) signaling in differentiation pathway of C2C12 myoblasts. *J. Biol. Chem.* **280**, 37660-37668.

Peifer, M. and Polakis, P. (2000). Wnt signaling in oncogenesis and embryogenesis-a look outside the nucleus. *Science* **287**, 1606-1609.

Rodda, S. J. and McMahon, A. P. (2006). Distinct roles for Hedgehog and canonical Wnt signaling in specification, differentiation and maintenance of osteoblast progenitors. *Development* **133**, 3231-3244.

Shen, R., Chen, M., Wang, Y., Kaneki, H., Xing, L., O'Keefe, R. J. and Chen, D. (2006a). Smad6 interacts with Runx2 and mediates Smurf1-induced Runx2 degradation. *J. Biol. Chem.* **281**, 3569-3576.

Shen, R., Wang, X., Drissi, H., Liu, F., O'Keefe, R. J. and Chen, D. (2006b). Cyclin D1-CDK4 induce Runx2 ubiquitination and degradation. *J. Biol. Chem.* **281**, 16347-16353.

Staal, F. J. and Clevers, H. (2000). Tcf/Lef transcription factors during T-cell development: unique and overlapping functions. *Hematol. J.* **1**, 3-6.

Tetsu, O. and McCormick, F. (1999). Beta-catenin regulates expression of cyclin D1 in colon carcinoma cells. *Nature* **398**, 422-426.

von Kries, J. P., Winbeck, G., Asbrand, C., Schwarz-Romond, T., Sochnikova, N., Dell'Oro, A., Behrens, J. and Birchmeier, W. (2000). Hot spots in beta-catenin for interactions with LEF-1, conductin and APC. *Nat. Struct. Biol.* **7**, 800-807.

Westendorf, J. J., Kahler, R. A. and Schroeder, T. M. (2004). Wnt signaling in osteoblasts and bone diseases. *Gene* **341**, 19-39.

Yu, H. M., Jerchow, B., Sheu, T. J., Liu, B., Costantini, F., Puzas, J. E., Birchmeier, W. and Hsu, W. (2005). The role of Axin2 in calvarial morphogenesis and craniosynostosis. *Development* **132**, 1995-2005.

Zeng, L., Fagotto, F., Zhang, T., Hsu, W., Vasicek, T. J., Perry, W. L., 3rd., Lee, J. J., Tilghman, S. M., Gumbiner, B. M. and Costantini, F. (1997). The mouse Fused locus encodes Axin, an inhibitor of the Wnt signaling pathway that regulates embryonic axis formation. *Cell* **90**, 181-192.

Zhang, M., Xie, R., Hou, W., Shen, R., Wang, X., Wang, Q., Zhu, T., Jonason, J. H. and Chen, D. (2009). PTHrP prevents chondrocyte premature hypertrophy by inducing cyclin D1-dependent Runx2 and Runx3 phosphorylation, ubiquitination and proteasome degradation. *J. Cell Sci.* **122**, 1382-1389.

Zhao, M., Harris, S. E., Horn, D., Geng, Z., Nishimura, R., Mundy, G. R. and Chen, D. (2002). BMP receptor signaling is necessary for normal murine postnatal bone formation. *J. Cell Biol.* **157**, 1049-1060.

Zhao, M., Qiao, M., Harris, S. E., Oyajobi, B. O., Mundy, G. R. and Chen, D. (2004). Smurf1 inhibits osteoblast differentiation and bone formation in vitro and in vivo. *J. Biol. Chem.* **279**, 12854-12859.

Zhu, M., Chen, M., Zuscik, M., Wu, Q., Wang, Y., Rosier, R. N., O'Keefe, R. J. and Chen, D. (2008). Inhibition of β-catenin signaling in articular chondrocytes results in articular cartilage destruction. *Arthritis Rheum.* **58**, 2053-2064.